

Isotopic constraints on lightning as a source of fixed nitrogen in Earth's early biosphere

Patrick Barth^{1,2,3,4*}, Eva E. Stüeken^{1,2}, Christiane Helling^{4,5}, Lukas Rossmann^{1,3,6}, Yuqian Peng², Wendell Walters^{7,8} and Mark Claire^{1,2}

^{1*}Centre for Exoplanet Science, University of St Andrews, North Haugh, St Andrews, KY16 9SS, UK.

²School of Earth & Environmental Sciences, University of St Andrews, Bute Building, Queen's Terrace, St Andrews, KY16 9TS, UK.

³SUPA, School of Physics & Astronomy, University of St Andrews, North Haugh, St Andrews, KY16 9SS, UK.

⁴Space Research Institute, Austrian Academy of Sciences, Schmiedlstrasse 6, Graz, A-8042, Austria.

⁵Fakultät für Mathematik, Physik und Geodäsie, TU Graz, Petersgasse 16, Graz, A-8010, Austria.

⁶School of Chemistry, University of St Andrews, North Haugh, St Andrews, KY16 9ST, UK.

⁷Institute at Brown for Environment and Society, Brown University, 85 Waterman St, Providence, 02912, Rhode Island, USA.

⁸Department of Earth, Environmental and Planetary Sciences, Brown University, 324 Brook St, Providence, 02912, Rhode Island, USA.

*Corresponding author(s). E-mail(s): pb94@st-andrews.ac.uk;

Abstract

Bioavailable nitrogen is thought to be a requirement for the origin and sustenance of life. Before the onset of biological nitrogen fixation, abiotic pathways to fix atmospheric N₂ must have been prominent to provide bioavailable nitrogen to Earth's earliest ecosystems. Lightning has been

2 *Isotopic constraints on lightning*

shown to produce fixed nitrogen as nitrite and nitrate in both modern atmospheres dominated by N₂ and O₂ and atmospheres dominated by N₂ and CO₂ analogous to the Archaean Earth. However, a better understanding of the isotopic fingerprints of lightning-generated fixed nitrogen is needed to assess the role of this process on the early Earth. Here, we present results from spark discharge experiments in N₂–CO₂ and N₂–O₂ gas mixtures. Our experiments suggest that lightning-driven nitrogen fixation may have been similarly efficient in the Archaean atmosphere, compared to modern times. Measurements of the isotopic ratio ($\delta^{15}\text{N}$) of the discharge-produced nitrite and nitrate in solution show very low values of -6 to -15% after equilibration with the gas phase with a calculated endmember composition of -17% . These results are much lower than most $\delta^{15}\text{N}$ values documented from the sedimentary rock record, which supports the development of biological nitrogen fixation earlier than 3.2 Ga. However, some Paleoproterozoic records (3.7 Ga) may be consistent with lightning-derived nitrogen input, highlighting the potential role of this process for the earliest ecosystems.

Keywords: Early Earth, Lightning, Nitrogen Isotopes, Origin of Life

On Earth, nitrogen is an essential building block for biological macromolecules such as DNA, RNA, and proteins and, therefore, must have been available for the origin of life and for the sustenance of early ecosystems. The most abundant form of nitrogen at the Earth's surface is atmospheric N₂ gas; however, this molecule is relatively inert, requiring dedicated nitrogenase enzymes or high energy to be converted into more bioavailable forms (nitrogen fixation). On the modern Earth, more than 97% of pre-industrial N₂ fixation is carried out by microorganisms; only a few percent of fixed nitrogen are produced by abiotic sources, the main source being lightning.^{1,2} On the early Earth, before the origin of life and the onset of biological N₂ fixation, these abiotic sources such as lightning must have been the dominant producer of bioavailable nitrogen. Lightning can occur when in a cloudy atmosphere cloud particles carry excess charges over long distances, building up large electric fields that eventually produce a lightning strike.³ Previous studies have shown that spark discharges produce nitrogen oxides in today's atmosphere^{4,5} as well as in N₂-CO₂-dominated atmospheres,^{6,7,8} and models suggest that a significant flux of these lightning products to the Earth's surface could potentially have fuelled prebiotic chemistry.^{9,10,11} However, it has so far not been possible to verify these model predictions and the role of lightning in the evolution of life, because the isotopic fingerprint of this nitrogen source was unknown, i.e. the ratio of the nitrogen isotopes ¹⁵N and ¹⁴N expressed as $\delta^{15}\text{N} = [({}^{15}\text{N}/{}^{14}\text{N})_{\text{sample}}/({}^{15}\text{N}/{}^{14}\text{N})_{\text{standard}} - 1] \times 1000 \%$, where the standard is modern air. In one laboratory experiment, values near 0% were reported from the gas phase.¹² However, natural measurements of atmospheric nitrate from different sources suggested values of -5% to -15% ¹³ with extreme

values between $< -30\text{‰}$ (nitrate and NO_x emission from the Antarctic snow-pack) and $> +5\text{‰}$ (fossil fuel emissions),¹⁴ indicating the wide range of sources of nitrate emissions on the modern Earth. Because experimental measurements of the aquatic phase have not yet been conducted, it has so far been impossible to detect evidence of lightning from the sedimentary rock record of nitrogen isotope ratios^{15,16,17} (Fig. 1).

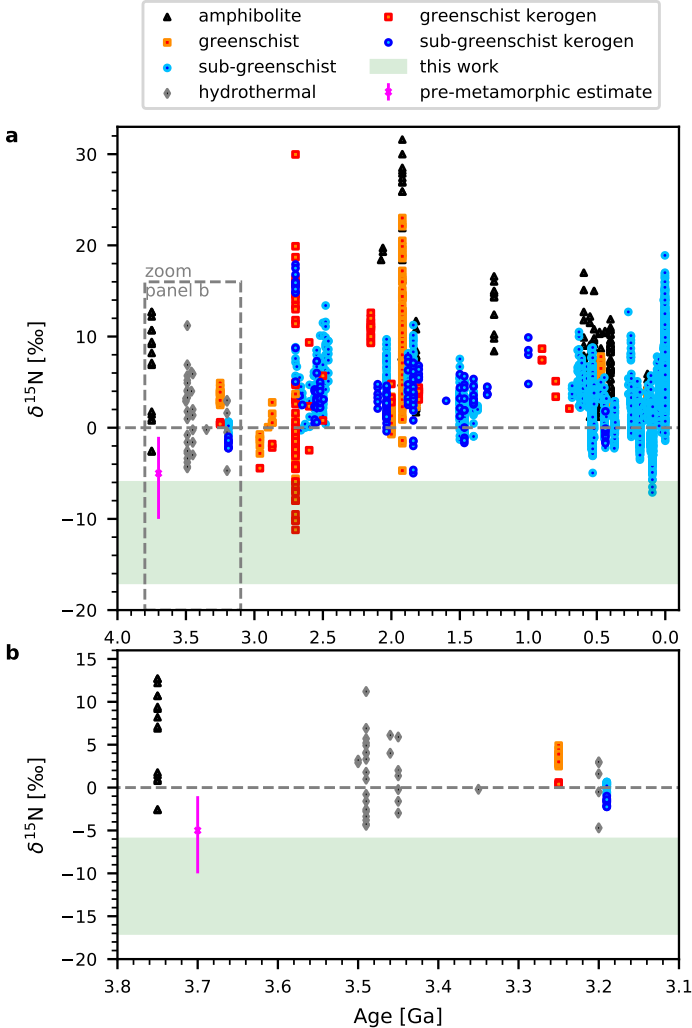


Fig. 1 Measurements of $\delta^{15}\text{N}$ in sedimentary rocks over geologic time, separated by metamorphic grade. **a**, Data from Stüeken et al.^{15,16} and Yang et al.¹⁷ Errors smaller than symbols. *Pink x*: pre-metamorphic estimate of 3.7 Ga old sample set (-5‰ , values between -1 and -10‰ possible).¹⁶ Our results after letting gas and water equilibrate are indicated by green shading. **b**, Zoom into area indicated in panel a by grey box.

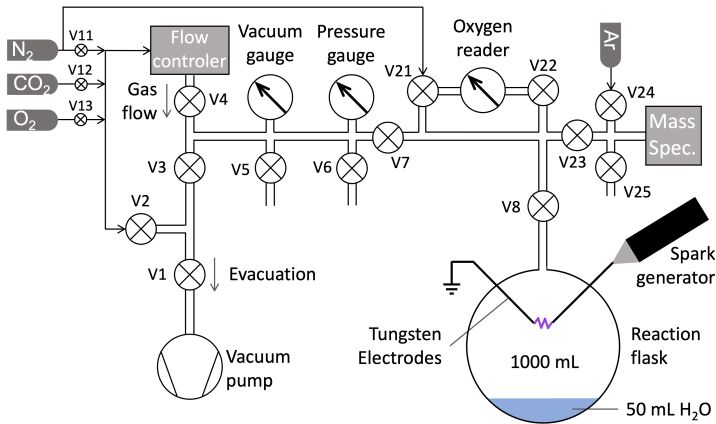
4 *Isotopic constraints on lightning*

Fig. 2 Schematic of experimental setup of the discharge experiment. See Methods for a detailed description of the procedure.

In this study we identified an isotopic fingerprint with spark discharge experiments in N₂–O₂ and N₂–CO₂ gas mixtures. We know from measurements of fluid inclusions that the isotopic composition of N₂ in early Earth’s atmosphere was very similar to today’s (within $\sim 2 - 3\%$),¹⁸ enabling us to compare our fingerprint to sedimentary rock samples. The experimental setup resembled a Miller-Urey apparatus¹⁹ with a 1 l glass flask and two needle electrodes at a distance of ~ 1.5 cm (Fig. 2). A current (*I*) of 1 mA at a voltage (*U*) of 49 kV was applied continuously for a time span (*t*) of 15 – 60 min per experiment. The flask was filled with artificial gas mixtures to 1 bar, mimicking modern (85% N₂, 14% O₂), O₂- and CO₂-depleted (99.5% N₂, 0.06% O₂, <0.02% CO₂), and Archean-like (83% N₂, 16% CO₂) atmospheres. For the CO₂ fraction in the Archean-like experiments we followed estimates predicting a CO₂ mole fraction of 15 to 20% in the early Archean.²⁰ In each case, 50 ml of deionized water at the bottom of the flask were used to trap soluble nitrogen oxides. Electrode spacing, energy input, experiment duration, fluid salinity and pH were varied and their effect on the results explored (see supplementary material). We measured the isotopic composition and abundances of these dissolved oxides by gas-source mass spectrometry, and the composition of the gas before and after the experiment using an on-line quadrupole gas analyser (see Methods). The molecular concentrations allowed us to determine energy yields (molecules/Joule), where energy input was calculated as $E = 1/2 UIt$. The energy yield could in turn be used to estimate global fluxes to the Earth’s surface for each of the major products. The isotopic composition allows us to test if lightning might have been an important nutrient source for early life.

Energy yield of nitrogen fixation

The main nitrogen product that is expected to form during spark discharges in N₂–O₂ and N₂–CO₂ gas mixtures is NO,^{9,21} which reacts further with

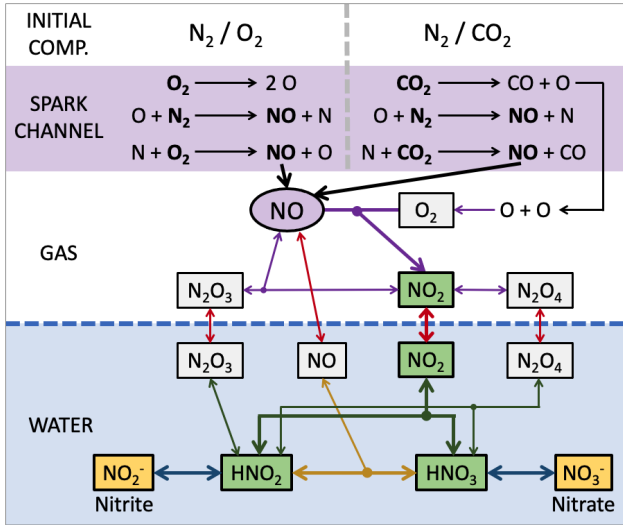


Fig. 3 Chemical pathways during spark discharge in N_2 – O_2 (left) and N_2 – CO_2 (right) gas mixtures. Once NO is produced, further oxidation follows the same reactions in both cases: NO is oxidised to NO_2 , some being converted to N_2O_3 and N_2O_4 . In N_2 – CO_2 experiments, O_2 is produced by the recombination of atomic oxygen. All gaseous nitrogen oxides equilibrate with water and convert to HNO_2 and HNO_3 . HNO_2 is thermodynamically unstable and will oxidise to HNO_3 . Both acids may dissociate to nitrite (NO_2^-) and nitrate (NO_3^-), respectively, depending on solution pH. In a low-pH environment, HNO_2 is more abundant than NO_2^- , allowing further oxidation to HNO_3 and nitrate. The dominant pathways are indicated with bold arrows and colored molecule labels.

O_2 to produce NO_2 and minor oxides (N_2O_3 , N_2O_4) (Fig. 3). In the anoxic experiments, the O_2 is provided by the recombination of atomic O after the dissociation of CO_2 .⁶ NO_2 dissolves into the water and converts to aqueous HNO_2 and HNO_3 , which in turn dissociate to NO_2^- and NO_3^- , respectively. Figure 4a shows the energy yield for the major products in our experiments for the different gas compositions. Yields for dissolved ammonium were also measured but found to be very low ($< 0.5\%$ of total fixed N) and are therefore not considered further, though our ammonium detection is consistent with previous observations of ammonium production in anoxic N_2 – CO_2 spark experiments.²² The modern and Archean-like scenarios both show a total energy yield for the sum of all fixed nitrogen species of $(3 - 5) \times 10^{15}$ molecules/J. Total yields are lower in the low- O_2 experiments, likely because NO formation was oxygen-limited. The speciation of the fixed nitrogen was found to vary with atmospheric composition: In the modern experiments (14% O_2), $\sim 85\%$ of the fixed nitrogen is stored in dissolved nitrate and nitrite. In the Archean-like experiments (16% CO_2), only about 50% is stored in nitrate and nitrite. The low- O_2 scenario yielded a smaller fraction of aqueous nitrogen species, nearly half of the fixed nitrogen remained in the gas phase. This suggests that in the Archean-like experiments the CO_2 provided enough oxygen for equally efficient NO formation as in an oxygen-rich atmosphere. However, O_2 availability appears to

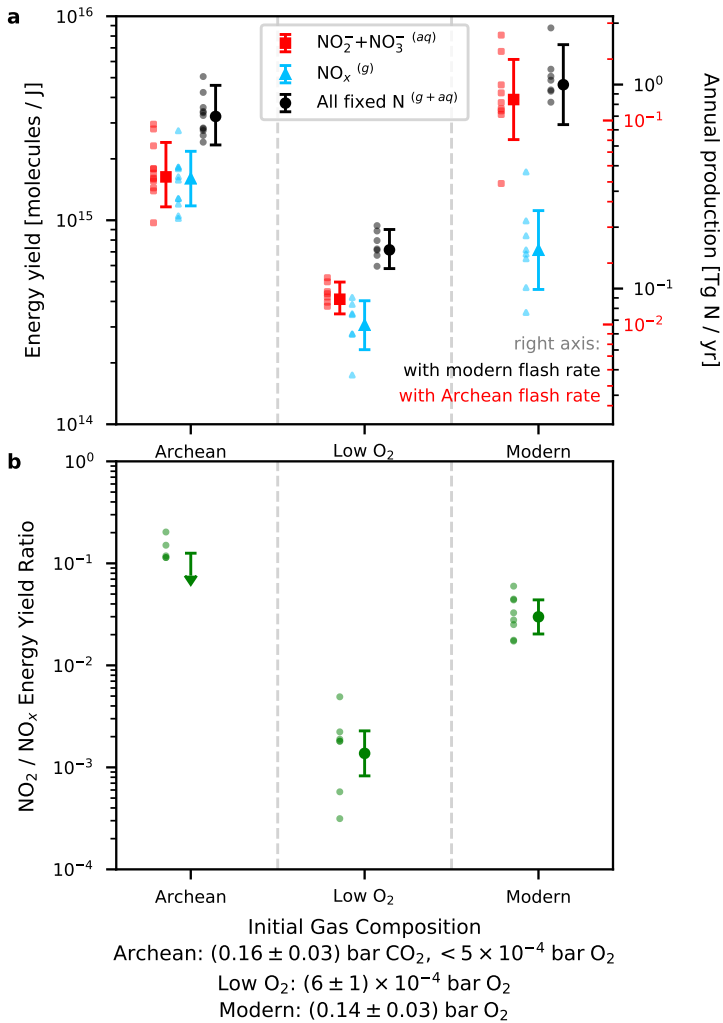


Fig. 4 Energy yield of fixed nitrogen products. **a**, Combined gaseous products (NO_x, blue), combined aqueous nitrate and nitrite (red), and total fixed nitrogen yield (black) for different initial gas compositions (difference to 1 bar is N₂). Individual measurements shown as small symbols, the large symbols represent the mean values (with SD error). Nitrite and nitrate are not separated, because nitrite conversion to nitrate was found to continue after the experiments. Right axis shows corresponding annual production for modern²³ (black) and potential Archean¹⁰ (red) lightning flash rates in Tg of fixed nitrogen per year. **b**, Ratio of the energy yields of NO₂ and NO_x for different initial gas compositions of the experiment (same as above). The data point for N₂-CO₂ gas represents only an upper limit due to interferences between NO₂ and CO₂ in the gas analyser.

limit the efficient conversion of NO to NO₂ and aqueous species. This interpretation is supported by the low NO₂/NO ratios measured in the low-O₂ experiment compared to the modern gas mixture (Figure 4b). Reliable NO₂

measurements for the Archean-like experiments could not be obtained due to interference between NO₂ and CO₂ isotopologues at mass 46, but the relatively low abundance of aqueous compared to gaseous products suggests that the Archean-like NO₂/NO ratio was also lower, due to oxygen-limitation.

To estimate global fluxes of fixed nitrogen to the Earth's surface, based on our results, we assumed a lightning flash rate in Earth's atmosphere²³ of $44 \pm 5 \text{ s}^{-1}$ and for the average energy dissipated by one lightning flash²⁴ of 6.7 GJ. Based on these assumption, our Archean-like and modern experiments predict the production of 0.7 – 1 Tg fixed nitrogen per year. A global lightning flash rate of only 6.6 s^{-1} ,¹⁰ as proposed for the Archean²⁵ would lower the annual fixed nitrogen production by lightning accordingly. The results are lower for the low-O₂ case (Fig. 4). Overall, these estimates are comparable to those of previous studies, including experiments that more closely mimic natural lightning conditions in terms of total energy input and spark length,^{26, 27, 28} supporting our approach of simulating lightning chemistry with small spark experiments. Previous experiments with a laser-induced plasma to simulate lightning discharge^{6, 7} found a 4-times lower NO energy yield (compared to our total fixed N yield) of 7×10^{14} molecules/J in N₂–CO₂ gas mixtures and a 20-times higher yield in modern air, compared to our measurements. However, it is uncertain how well a laser can mimic lightning chemistry. In a natural lightning channel, gas is heated within a few microseconds to a peak temperature of 30 000 K.^{29, 30} The gas cools to ~ 3000 K over a few to tens of milliseconds.^{31, 32} While the gas is cooling NO forms. However, the timescales for thermochemical equilibrium to establish increases with further cooling from microseconds at 4000 K to 1000 yr at 1000 K,³³ causing the NO concentration to be fixed once the cooling time-scale drops below the equilibrium time-scale.³⁴ Hence, even though in our experiments the spark channel does not reach the temperature of a fully-developed lightning channel, NO was still observed to be the dominant product, which allows us to mimic natural atmospheric chemistry induced by lightning. To further verify the validity of our results for natural settings, we ran a subset of experiments with artificial seawater and CaCO₃ as a pH buffer (see supplementary material), and found no effect on the nitrite concentrations, indicating that our results are valid for both fresh and saline water. Experiments with anoxic seawater and 0.8 mM ferrous iron, akin to the Archean ocean,³⁵ had similar yields, suggesting that potential reactions between nitrogen oxides and ferrous iron³⁶ are relatively minor and do not impact our conclusions.

Isotope fractionation during spark experiment

We analysed the nitrogen isotopic composition in the dissolved oxides with two different techniques (see Methods). For most experiments, the solutions were mixed with KOH powder, freeze-dried, and then analysed as dried salt. For a subset of experiments, dissolved nitrate and nitrite were treated with the denitrifier method and analysed as N₂O gas^{37, 38} which allowed separating

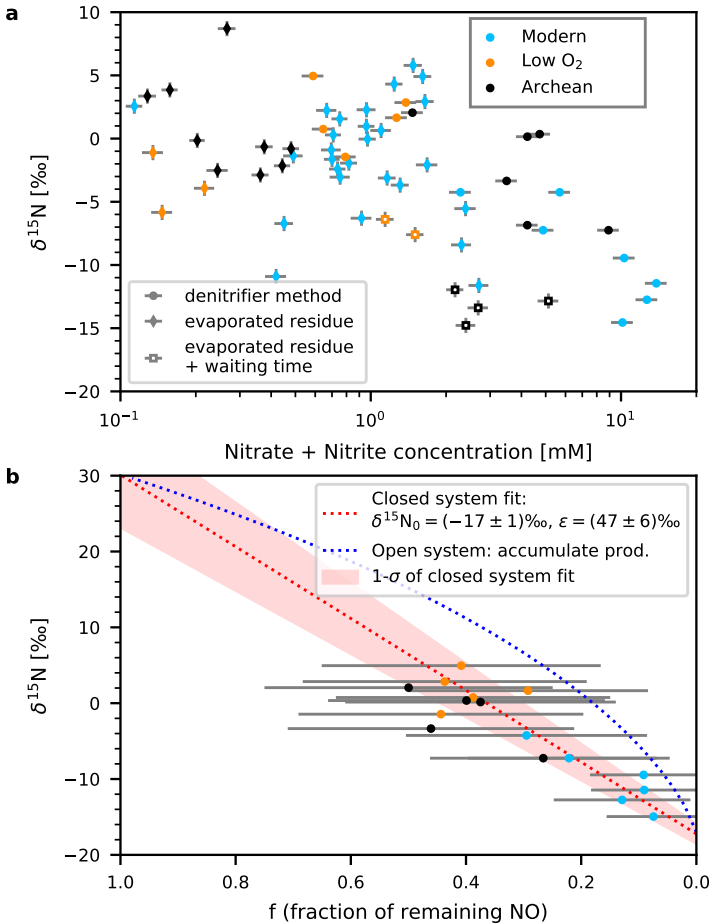


Fig. 5 Nitrogen isotope ratios of aqueous nitrate and nitrite. **a**, $\delta^{15}\text{N}$ against combined concentration of nitrate and nitrite in mM (10^{-3}mol/l). Data from three sets of experiments (symbol shape) and three gas mixtures (symbol color). Data points are individual measurements with uncertainties in concentration and $\delta^{15}\text{N}$ (errors in $\delta^{15}\text{N}$ for denitrifier method smaller than symbols). **b**, $\delta^{15}\text{N}$ against remaining fraction of NO $f = [\text{NO}]/([\text{NO}] + [\text{NO}_2] + [\text{NO}_2^-] + [\text{NO}_3^-])$. NO abundances to calculate f only available for experiments analysed with the denitrifier method (circles). Dashed red line is fit to a closed system Rayleigh fractionation ($\delta^{15}\text{N}(f) = \delta^{15}\text{N}_0 + \epsilon f$) with $1\text{-}\sigma$ envelope, allowing to extrapolate to endmember where all NO oxidised to nitrate and nitrite. Blue line represents the $\delta^{15}\text{N}$ of the accumulated product in a Rayleigh fractionation assuming an open system with same $\delta^{15}\text{N}_0$ and ϵ as closed system. See text for discussion of open and closed system fractionation. Data points represent individual measurements with error in f propagated from uncertainties of the measurements of the individual concentrations (NO , NO_2 , NO_2^- , NO_3^-).

out other nitrogen compounds such as ammonium. The two datasets combined define an overlapping trend of progressively more negative $\delta^{15}\text{N}$ values with higher combined nitrate and nitrite concentrations, with values as low as

−15‰ (Fig. 5a). Neither of the two methods was able to separate nitrite from nitrate, which is why we report them together.

Combined with the gas data, we find that the isotopic composition decreases as the fraction of NO remaining in the gas phase $f = [\text{NO}]/([\text{NO}] + [\text{NO}_2] + [\text{NO}_2^-] + [\text{NO}_3^-])$ decreases (Fig. 5b). The extrapolated endmember composition with 0% NO remaining is $\delta^{15}\text{N}_0 = -17 \pm 1\%$, the initial $\delta^{15}\text{N}$ of the NO reservoir, with an ϵ factor (i.e. the fractionation between the NO reservoir and the first produced nitrate) of $47 \pm 6\%$. We used a linear fit as our experiment can be described by a closed system Rayleigh fractionation where the initial reservoir and the accumulated products remain in contact as supported by further experiments where the flask was let sit idle for several hours after the end of the experiment, leading to even lower values for $\delta^{15}\text{N}$ (open squares in Fig. 5a) than in experiments with no additional rest time (circles). In natural lightning clouds, we might find some open-system behavior when large rain droplets escape from the system. However, the fractionation in an open system is very similar to that of our closed system experiments as we would start with the same $\delta^{15}\text{N}_0$ and ϵ (blue line in Fig. 5b).

Theoretical calculations of equilibrium isotope fractionation have shown that NO gas should be isotopically depleted relative to N_2 and NO_2 .³⁹ Very light $\delta^{15}\text{N}$ values (−15 to −25‰) have also been measured in organic particulates forming in spark discharge experiments,⁴⁰ consistent with significant isotopic fractionation occurring in lightning chemistry. Hence the following sequence of events is the most logical explanation for the trend in our data: First, isotopically light NO ($\delta^{15}\text{N}$ near −17‰) is produced in the gas phase. Our extrapolated endmember for NO ($\delta^{15}\text{N}_0 = -17 \pm 1\%$) falls close to the value predicted for the kinetic isotope fractionation in the reaction $\text{N}_2 + \text{O} \longrightarrow \text{NO} + \text{N}$, $\epsilon = -17.4\%$,⁴⁰ resulting from the higher velocity and increased reaction rate of $^{14}\text{N}^{14}\text{N}$ compared to the heavier $^{15}\text{N}^{14}\text{N}$. Second, some NO is converted to NO_2 with a positive fractionation, i.e. isotopically heavy NO is preferentially converted to NO_2 . Previous studies have reported nitrogen enrichment factors of 29‰⁴¹ to 36‰⁴² between these two species, with additional, minor fractionation possible between gaseous and aqueous NO_2 . Since we find efficient conversion of NO_2 to nitrite and nitrate, the final isotopic composition of these products is very similar to the $\delta^{15}\text{N}$ of the NO_2 . When only a small fraction of NO has been converted (high f -value in Fig. 5b), the isotopic composition of nitrate and nitrite falls near 20‰. Third, progressive conversion of isotopically heavy NO to aqueous species (via NO_2) renders the residual NO gas phase isotopically lighter. Hence, nitrite and nitrate forming at a larger conversion factor (a smaller f in Fig. 5b) become isotopically lighter as well.

This is supported by our experiments with additional wait time, allowing more NO to convert to aqueous species over time. The system trends over time towards an equilibrium with isotopically light aqueous species (−6 to −15‰ and possibly lighter, given more time). In our experiments, the equilibration time is likely to be affected by diffusion kinetics between the gas and the water

reservoir. In a natural lightning storm in a water-saturated atmosphere, the equilibration between gaseous NO and aqueous nitrite and nitrate is likely to be reached faster, possibly leading to even lower $\delta^{15}\text{N}$ values trending towards the depleted lightning-generated $\delta^{15}\text{N}(\text{NO})$.

Quantifying lightning as a source of nitrogen for early life

It has long been postulated that lightning may have driven the origin and early evolution of life on Earth, based on estimates of fluxes and biological demands.^{9,6,7,10} In this work we find that nitrogen fixation in an Archean-like ($\text{N}_2\text{--CO}_2$) atmosphere is similarly efficient to a modern ($\text{N}_2\text{--O}_2$) atmosphere, but further oxidation of NO to nitrite and nitrate is limited by the absence of O_2 . The overall production of fixed nitrogen products depends on the Archean lightning flash rate which might have been lower than today's.¹⁰ There is still significant uncertainty relating to the CO_2 fraction in the early Archean atmosphere²⁰ which will influence the final nitrogen fixation rate.⁶ An additional uncertainty is the total atmospheric pressure in the Archean, where estimates vary between 0.5¹⁸ and 3 bar.⁴³ The velocities of the electrons inside the spark channel, responsible for the dissociation of N_2 , O_2 , and CO_2 , are independent from the gas density, i.e. the pressure.⁴⁴ However, the three-body reactions outside the spark channel depend on the gas number density. To check whether our results are still valid for different atmospheric pressures, we used simulations with the chemical kinetics network STAND2019^{45,46,47} to compare the NO_2 production outside the spark channel (at 300 K) for pressures of 0.5, 1, and 3 bar. The final NO_2 fraction varied between approximately 80% (for 0.5 bar) and 140% (for 3 bar) compared to 1 bar (our experiments) where we find an NO_2 mixing ratio of 2.8×10^{-5} . This uncertainty is much smaller than other factors that influence the NO_2 production rate such as the initial CO_2 fraction in the atmosphere or the lightning flash rate on the early Earth. A further factor of uncertainty is the availability of O_2 for the production of NO_2 in the Archean atmosphere. When O_2 is formed by the recombination of atomic oxygen outside of the spark channel, it will be diluted in the background gas. While our experiments present a limited gas volume in which the chemistry takes place, in real lightning conditions, the O_2 could be transported away from the thunderstorm cloud, reducing the efficiency of NO_2 production. We expect the production of NO_2 to happen relatively quickly while the gasses are still in the vicinity of the lightning channel, but kinetic rate modeling is necessary to answer this question definitively.

Our isotopic data allow us to place first empirical constraints on the role of lightning-derived bioavailable nitrogen in the early evolution of life. We find the dissolved lightning products significantly lighter ($\delta^{15}\text{N} = -6$ to -15‰ or less) than the vast majority of sedimentary rocks through geologic time (Fig. 1). This conclusion holds when corrected for metamorphic alteration, which is around 1 – 2‰ at greenschist facies,⁴⁸ applicable to most samples

in the compilation. $\delta^{15}\text{N}$ values significantly below -5‰ have been documented from one site in the Neoproterozoic,¹⁷ interpreted as evidence of high ammonium availability. No other settings display such light values, making it unlikely that lightning was a significant source of nitrogen to the biosphere for most of Earth's history. It is possible that atmospheric products would have undergone further fractionation after raining out into the ocean, such that the residuum became isotopically heavier and was subsequently trapped in biomass. However, such fractionating processes would deplete the nitrite and nitrate reservoir, making it unlikely that sufficient fixed nitrogen remains in solution to support the ecosystem. Similarly, UV photolysis can reduce the nitrate and nitrite concentration in the ocean, limiting the contribution to the ecosystem.⁴⁹

Another source of fixed nitrogen on early Earth could have been photochemical production of HCN due to UV irradiation of the atmosphere.⁵⁰ However, on Titan, where UV radiation and cosmic rays produce a significant amount of HCN, the nitrogen in the HCN is very heavily enriched in ^{15}N compared to the N_2 ($\delta^{15}\text{N}$ values of $\sim 4000\text{‰}$ (for HCN, ref⁵¹) and $\sim 650\text{‰}$ (for N_2 , ref⁵²), respectively). If photochemical HCN production had been a significant source of nutrients on the early Earth, we would expect to see a strong enrichment of ^{15}N in the rock samples.

Our results are thus consistent with the notion that biological N_2 fixation evolved early,⁵³ making the biosphere independent from lightning as a nutrient source. There is, however, potentially one exception, that we know of, of rocks from the Paleoproterozoic, where reconstructed pre-metamorphic $\delta^{15}\text{N}$ values may have been as low as -10‰ (ref,¹⁶ pink line in Fig. 1). If correct, those numbers could represent a lightning contribution, meaning that Earth's earliest ecosystems and by extension prebiotic networks may have benefitted from lightning reactions.

To conclude, our results suggest that lightning was not the main source of bioavailable nitrogen for the established biosphere, but it could have been significant for Earth's earliest ecosystems and possibly for life's origins. In addition, our results allow the community to investigate the source of fixed nitrogen on other bodies in the Solar System such as Mars where the Mars Science Laboratory and subsequent measurements have detected deposits of nitrate in several locations.^{54, 55}

Acknowledgments. We thank Henderson (Jim) Cleaves for technical advice on the experimental setup, Paul Rimmer and the members of the Leverhulme Centre for Life in the Universe (Cambridge) for helpful discussions of our results, and Ben K. D. Pearce for comments on our manuscript. P.B. acknowledges a St Leonard's Interdisciplinary Doctoral Scholarship from the University of St Andrews. E.E.S. acknowledges funding from a Royal Society research grant (RGS\R1\211184) and from a NERC Frontiers grant (NE/V010824/1). Ch.H. is part of the CHAMELEON MC ITN EJD which received funding from the European Union's Horizon 2020 research and innovation programme under the Marie Skłodowska-Curie grant agreement number 860470. In order to

meet institutional and research funder open access requirements, any accepted manuscript arising shall be open access under a Creative Commons Attribution (CC BY) reuse licence with zero embargo. This version of the article has been accepted for publication after peer review but is not the Version of Record and does not reflect post-acceptance improvements or any corrections. The Version of Record is available online at <https://doi.org/10.1038/s41561-023-01187-2>.

Authors' contributions. E.E.S. and Ch.H. conceived the project; E.E.S. and P.B. built the experimental setup; P.B., L.R. and Y.P. carried out the experiments; P.B., L.R., Y.P. and W.W. performed the analyses; M.C. provided analytical support; P.B., E.E.S., Ch.H. and W.W. analysed the data; P.B. wrote the manuscript with contributions from all authors.

Competing interests. The authors declare no competing interests.

Methods

Experimental setup

All experiments were carried out at the University of St Andrews in the St Andrews Isotope Geochemistry Lab (StAIG). We used an experimental setup similar to the one described by Parker et al.¹⁹ (Fig. 2). The spark discharge was contained in the 1-litre reaction flask (Pyrex glass), which contained both the water and the spark electrodes (tungsten metal). This flask was connected to a vacuum line (stainless steel) with an ultra-torr fitting and thus could be disconnected at the end of the experiment. The sparks were generated by a *BD-50E Heavy Duty Spark Generator* with a maximum voltage of 49 kV. Before starting an experiment, the system was evacuated by opening V1 and V3 to the vacuum pump. The valve to the reaction flask (V8) was only opened once the rest of the line was evacuated to minimize evaporation of water from the experimental flask. Once the pressure within the flask had reached a few mbar, V3 and V1 were closed and the system was filled with N₂ gas via V2 up to 1 bar pressure. The N₂ was re-evacuated, and this process was repeated 2 times to completely purge the reaction flask. After that, the desired gas mixture was introduced. Originally, we aimed for O₂ concentrations of 21% and 1% for the modern and low-O₂ experiments, respectively, and a CO₂ concentration of 20% for the Archean-like experiments. However, slow mixing of the gasses in our the set-up led to slightly lower final concentrations of CO₂ and O₂: Archean-like: 0.16 ± 0.03 CO₂ and $< 5 \times 10^{-4}$ O₂; Low-O₂: $< 2 \times 10^{-4}$ CO₂ and $(6 \pm 1) \times 10^{-4}$ O₂; Modern: $< 6 \times 10^{-4}$ CO₂ and 0.14 ± 0.03 O₂. The small amounts of CO₂ present in the modern and low-O₂ experiments and of O₂ in the Archean-like experiments is likely due to these gasses being dissolved in the water and not completely removed during evacuation, traces of air remaining in the setup, and recombination of atomic oxygen produced by dissociation of H₂O and CO₂ in the experiment and the ion source of the mass spectrometer. For the O₂ in the low-O₂ experiments, we used a flow controller (Bronkhorst EL-FLOW Prestige). Before starting the spark discharge,

valve V8 was closed to disconnect the reaction flask from the rest of the setup. An oxygen sensor was used to monitor the trace amount of oxygen present in anoxic experiments. Before and after each experiment, the gas from the flask was allowed to flow towards a quadrupole mass spectrometer gas analyser via V23 (see below for analytical method). We did not perform gas analyses during the experiment, because we found that a larger reservoir of NO and NO₂ needed to be generated before reliable measurements could be made. When not connected to the experiment, argon gas was fed to the mass spectrometer via V24 and V25 to keep the system free from contaminants. After the experiment, the fluid phase was transferred into a 50ml Falcon centrifuge tube for subsequent analyses (see below).

NO_x gas abundance measurements

Before and after the spark experiment, the gas composition in the flask was analysed with a quadrupole mass spectrometer (Hiden Analytical ExQ Quantitative Gas Analyser) to determine the abundance of all gases, including NO and NO₂. The instrument was run in *Multiple Ions Detection* mode to monitor the abundance of several mass/charge ratios (m/z) (12, 14, 15, 16, 17, 18, 20, 28, 30, 32, 40, 46, 48) and thus detect N₂, O₂, CO₂, NO, N₂O, NO₂, and O₃. When analysing the pure N₂-O₂ gas before running the spark experiment, a peak at m/z 30 was detected. This is likely due to the recombination of ¹⁴N and ¹⁶O fragments from the N₂ and O₂, respectively, to NO inside the mass spectrometer.⁵⁶ By comparing measurements from before and after the spark experiment, this interference could be subtracted. We found these background measurements to be very stable with variations in the background between 3% and 17% for the Archean-like and modern experiments, respectively. We also measured and subtracted the background for the other masses and used the standard deviation of these background measurements for the error of our gas measurements. However, after combining multiple measurements for Fig. 4, the standard deviation of this average is substantially larger than the combined individual errors which scale with $1/\sqrt{N}$ for N data points.

To determine the molecular abundances from the measured intensities, we used the mass spectra provided in the NIST database,⁵⁷ which accounts for fragmentation of molecules in the ion source of the instrument. Unfortunately, N₂O produced signals at m/z 30 and 44, overlapping with peaks for NO and NO₂ at m/z 30, and CO₂ at m/z 44. However, calculations and experiments suggest that N₂O production in lightning and discharge experiments is approximately 4 magnitudes lower than NO production,^{58,59} suggesting that the contribution of N₂O to the peak at m/z 30 can be neglected. The abundance of NO₂ could be determined by the signal intensity of the m/z 46 peak; the abundance of NO from m/z 30 after subtracting the contribution by the NO-fragment from NO₂. For experiments with a high CO₂ abundance, the CO₂ isotopologue ¹⁶O¹²C¹⁸O also contributes to the m/z 46 peak. We tried to subtract this interference, but the uncertainty is relatively large. The data from the CO₂-rich experiments therefore only gave us an upper limit of the NO₂

concentration (see Fig. 4). We also found trace amounts of ozone (m/z 48) of $\sim 8 \times 10^{-7}$ bar in the N_2 - CO_2 experiments and $\sim 4 \times 10^{-5}$ bar in the modern atmosphere experiments, with the detection limit being $\sim 10^{-7}$ bar (100 ppb).

Aqueous nitrate and nitrite analyses

To determine the concentrations of nitrate (NO_3^-) and nitrite (NO_2^-) in our solutions, we used an Metrohm 930 *Ion Chromatograph* (IC) with a Metrohm 919 autosampler, a 150 mm Metrosep A Supp 5 separation column (4 mm bore) with 3.2 mM Na_2CO_3 / 1 mM $NaHCO_3$ anion eluent at a flow rate of 0.7 ml min^{-1} . We ran it using a Metrohm Suppressor Module with a phosphoric and oxalic acid eluent suppressor solution.

The subset of samples shipped to Brown University was analyzed for NO_2^- and NO_3^- using colorimetric and IC analytical techniques. The concentrations of NO_2^- were determined using a standardized colorimetric technique (e.g., US EPA Method 353.2) involving the diazotization with sulfanilamide dihydrochloride followed by detection of absorbance at 520 nm that was automated using a discrete UV-Vis spectrophotometer (Westco SmartChem). The analysis of NO_3^- concentrations was conducted using a reagent-free Dionex Integrion HPIC System with a Dionex AS-HV Autosampler, Dionex AG19 guard and analytical columns, with 20 mM KOH anion eluent at a flow rate of 1 ml min^{-1} .

The nitrite and nitrate concentrations in the experiments with different water compositions (see supplementary material) were measured with a colorimetric method using vanadium(III) chloride as a reduction agent.⁶⁰ Analyses were performed with a Thermo Fisher Evolution 220 Computer Control UV-Vis Spectrophotometer with wavelengths set to 530nm for nitrite and 560nm for nitrate. This method was used instead of the IC to avoid overloading the IC column with chloride.

Ammonium concentrations were measured by colorimetry, following the method by Solorzano et al.⁶¹ as described by Cleaves et al.²² After mixing with the appropriate amount of reagents, the solutions were analysed at 640 nm with a Thermo Fisher Evolution 220 Computer Control UV-Vis Spectrophotometer. We found the detection limit of this method to be at 3.4 μM .

Nitrogen isotope measurements

For the ‘evaporated residue’ method, carried out at the University of St Andrews, 40 ml of each water sample were mixed with 250 mg of KOH to form KNO_3 and KNO_2 . This solution was then evaporated with a freeze drier for about one week until the residue was completely dry. The dried residue was weighed into tin capsules and analysed by flash-combustion, using an *elemental analyser* (EA IsoLink) coupled to an *isotope ratio mass spectrometer* (MAT253 Thermo Finnigan) via a ConFlo IV. The analyses were calibrated with the international reference materials RM8568/USGS34 ($\delta^{15}N = -1.8\text{‰}$; $\delta^{18}O =$

−28‰), RM8569/USGS35 ($\delta^{15}\text{N} = 2.7\text{‰}$; $\delta^{18}\text{O} = 57\text{‰}$), RM8549/IAEA-NO-3 ($\delta^{15}\text{N} = 4.7\text{‰}$; $\delta^{18}\text{O} = 25.6\text{‰}$).^{62, 63, 64} We note that adding KOH to the sample increases the pH of the solution, which includes small amounts of NH_4^+ . Once the pH is increased above 9.25, most NH_4^+ will dissociate to NH_3 which can be lost by volatilisation with a fractionation of -45‰ .^{65, 15} Tests to quantify this effect on the bulk measurement of the nitrogen isotope fractionation showed that the ammonium concentration was too small for any volatilisation to affect the measured bulk isotopic value. A subset of samples was also analyzed for nitrogen and oxygen isotope composition at Brown University using the denitrifier method.^{37, 38} Briefly, samples were injected into vials containing *P. aureofaciens* that quantitatively convert nitrate and nitrite to nitrous oxide (N_2O). The generated N_2O was concentrated and purified using an automatic purge and trap system and introduced to a continuous flow isotope ratio mass spectrometer with a modified gas bench interface. Measurement of N_2O was conducted at an m/z of 44, 45, and 46 for $\delta^{15}\text{N}$ and $\delta^{18}\text{O}$ determination, and unknowns were corrected relative to internationally recognized nitrate salt reference materials that included: USGS34, USGS35, and IAEA-NO-3 (see above). Both methods return the combined isotopic compositions of nitrate and nitrite.

Kinetic chemistry calculations

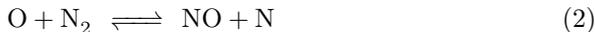
To test how the production of NO_2 depends on atmospheric pressure, we performed calculations with the photochemistry and diffusion code ARGO and the chemical kinetics network STAND2019.^{45, 46, 47} STAND2019 contains 3085 forward reactions of 224 charged and 197 neutral species. For the starting conditions, we assumed that 1% of the gas mixture was cycled through the spark in our experiments. We further assumed that the composition of this portion of the gas corresponds to the chemical equilibrium composition of the initial gas mixture (84% N_2 , 15% CO_2 , 1% H_2O) at a freeze-out temperature of 3000 K. We calculated the chemical equilibrium composition at 3000 K with GGChem,⁶⁶ including 87 neutral and charged species containing the elements H, C, N, O, as well as electrons. We then added the calculated concentrations of H, N, O, H_2 , N_2 , O_2 , OH, NO, CO, CO_2 , H_2O (in total 1%) to the background gas (99%) and used this total gas mixture as input for ARGO/STAND2021. We performed the kinetic chemistry simulations at a temperature of 300 K and pressures of 0.5, 1, and 3 bar and compared the resulting NO_2 concentrations when steady state was reached after 69, 23, and 3 min at 0.5, 1, and 3 bar, respectively. Increasing the fraction of gas cycled through the spark channel does not affect the ratio between the NO_2 concentrations for the different gas pressures, but decreases the time scale to reach steady state.

Data availability. A full methods section, a detailed description of the chemical processes, the description of additional experiments, and a machine-readable table of the data presented in this work is available online. To access the data please follow <https://doi.org/10.5285/81dfa4de-5a47-479f-8de8-15e5ef398072>.

Supplementary Material

Chemical pathways

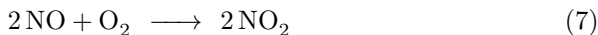
The production of NO in the spark channel follows the Zel'dovich mechanism³⁴ with the following reactions in a N₂–O₂ atmosphere:^{5,33}



Similar reactions lead to the production of NO in a N₂–CO₂ atmosphere:⁶



In addition, atomic oxygen will recombine to form O₂. A schematic showing the chemical reactions in our experiment is shown in Fig. 3. In both gas compositions, the NO will then oxidise further to NO₂, which will be in equilibrium with N₂O₃ and N₂O₄.^{67,21}

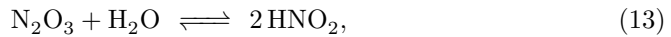
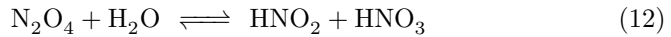
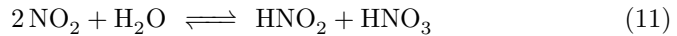


Another potential product of further reactions involving NO is N₂O. However, discharge experiments⁵⁸ found that the yield of N₂O is about 4 magnitudes lower than that of NO,⁶⁸ 4×10^{12} molecules/J and 5×10^{16} molecules/J, respectively. Theoretical calculations⁵⁹ return an even slightly lower N₂O yield of 8×10^{11} molecules/J. We therefore neglected any N₂O production in our analysis. NO can also react to NO₂ in the presence of ozone. We did measure low ozone concentrations in some of our experiments but it is uncertain how important this pathway is here. The gas mixture in our experiments contains approximately 1% of water vapour due to evaporation of the liquid water in the flask at room temperature, which limits the abundance of ozone in the gas mixture.⁶⁹ In anoxic conditions, Summers et al.⁷⁰ have shown that the disproportionation reaction

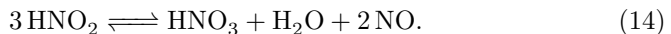


is an important source of NO₂. However, in their experiments, NO was introduced directly into a gas mixture of N₂ and CO₂, meaning no spark is present that could provide O₂ from CO₂ and H₂O dissociation for NO₂ production via Reaction (7).

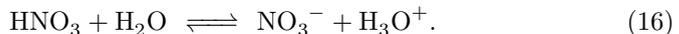
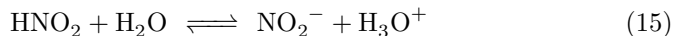
NO_2 , N_2O_3 , and N_2O_4 , will be absorbed into the water (in equilibrium with the partial pressure in the gas) where they will further react with the water to HNO_2 and HNO_3 .^{67, 21}



HNO_2 is not stable and will further react to HNO_3 ,



HNO_2 and HNO_3 will further react with water to nitrite (NO_2^-) and nitrate (NO_3^-), respectively:



In a low pH environment (Fig. S6), HNO_2 is more abundant than NO_2^- , allowing further oxidation to HNO_3 and nitrate. We found that the nitrite concentrations in our samples were systematically lower if the analyses were performed several days after the experiment rather than on the same day, suggesting that nitrite was continuously converted to nitrate in the aqueous phase. We speculate that this is due to the presence of another strong oxidizer produced in the spark experiment, such as H_2O_2 , which is known to be produced by lightning.⁷¹ Our oxygen isotope data ($\delta^{18}\text{O}$ has a consistent value of 20 ‰ throughout all experiments) further supports this pathway of nitrate formation via nitrite: In acidic conditions (our solutions have a $\text{pH} < 4$, see Fig. S6), nitrite exchanges oxygen with water, completely eradicating the isotopic signature of the initial nitrite.^{72, 73}

The dominant pathway for nitrate formation is indicated in Fig. 3 with bold arrows and goes via Reaction (10). Even for our experiments where the final NO_2 pressure is largest, both N_2O_3 and N_2O_4 pressures are approximately 4 orders of magnitude smaller than the overall NO_x pressure when using the equilibrium constants.⁶⁷ Since the final partial pressure of NO_2 is below 1 mbar in all our experiments, NO_2 absorption is the most important route of nitrate formation, as opposed to N_2O_4 absorption.^{67, 74}

Additional experiments

We tested the influence of the electric field strength on the production of nitrite and nitrate. The field strength depends on the applied voltage and the size of the gap between the electrodes. We used an approximation of the electrodes by long and thin ellipsoids⁷⁵ but could not find a clear correlation to the nitrate production.

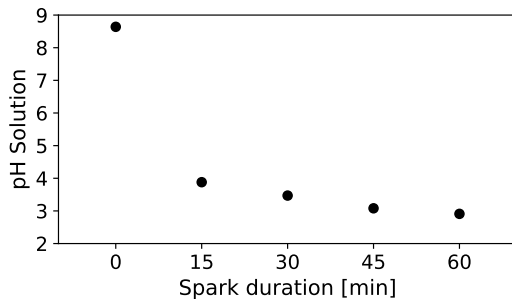


Fig. S6 pH of solution at different times during spark experiments. Starting with 50 ml DI water, gas: 0.9 bar N_2 and 0.1 bar CO_2 .

Spark gap effects

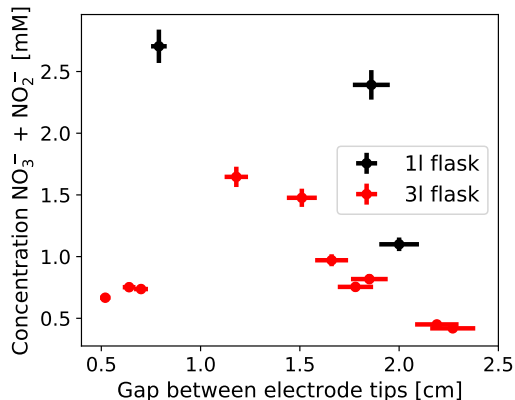


Fig. S7 Final Concentration of Nitrate + Nitrite for experiments with varying distance between the electrode tips. Only experiments with modern atmospheric composition. Experiments performed with a 1l and 3l flask are shown in black and red, respectively. Data points are individual measurements with uncertainties in concentration and distance.

However, experiments with differently sized spark gaps showed an interesting behaviour (Fig. S7). For large spark gaps, the production of nitrate and nitrite dropped as the electric field strength approached the breakdown field in dry air⁷⁶ of 35 kV cm^{-1} and the continuity of the spark was disturbed. On the other hand, with a decreasing spark gap, the total volume of the spark channel decreased which in return limited the degree of nitrogen fixation, possibly because a larger portion of the energy was lost as heat to the electrodes. We identified a setting where the nitrate production peaked for spark gaps between 1 cm and 1.5 cm which we used for all further experiments. Note that some of the initial experiments were carried out with a 3l flask, but we transitioned to a 1l flask for the majority of the project, because this allowed for a

more efficient absorption of the produced nitrogen oxides into the water as the partial pressures of NO and NO₂ were relatively higher in the smaller volume. Furthermore, the 1 l flask was faster to evacuate.

Energy yield

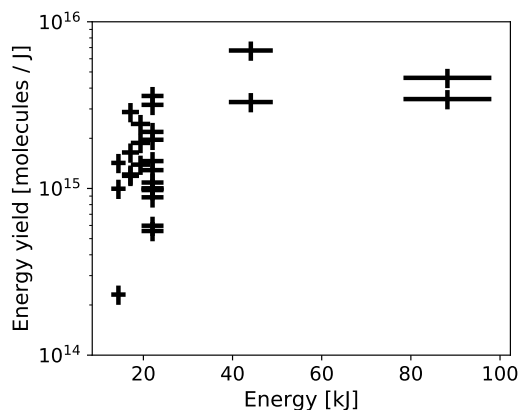


Fig. S8 Energy yield (N atoms fixed per Joule) against input energy for production of Nitrate + Nitrite. Only experiments with modern atmospheric composition. Data points are individual measurements with uncertainties in energy and energy yield.

The rate of nitrogen fixation increases with increasing energy. The energy input into the experiment can be calculated with the voltage U and current I of the spark generator and the duration t of the spark: $E = 1/2 UIt$. The voltage can be changed in increments with $U_{max} = 49 \pm 2$ kV and the current is $I = (1 \pm 0.1)$ mA. The duration of the spark ranged between 15 and 60 min. The energy yield (nitrate and nitrite) increases with increasing energy, levelling off above approximately 40 kJ (Fig. S8). Reasons for the less efficient production of nitrate and nitrite at lower energies are likely a combination of higher energy losses by heating of the electrodes and less time for further oxidation of NO_x to nitrate and nitrite as the low-energy experiments typically represent spark durations of 15 min.

Effects of duration and water composition

A subset of experiments was designed to compare the effect of simulated modern and early Archean seawater on the yields of nitrite, nitrate, and ammonium in the discharge experiments with a constant gas composition of 0.9 bar N₂ and 0.1 bar CO₂ to simulate an anoxic neutral Earth's early atmosphere. Four different liquid compositions⁷⁷ were used: (1) DI water (2) Modern seawater (3) Modern seawater with CaCO₃ buffer (4) Archean seawater. First, 500 ml of the solution were prepared in a volumetric flask (see Table S1) and the initial

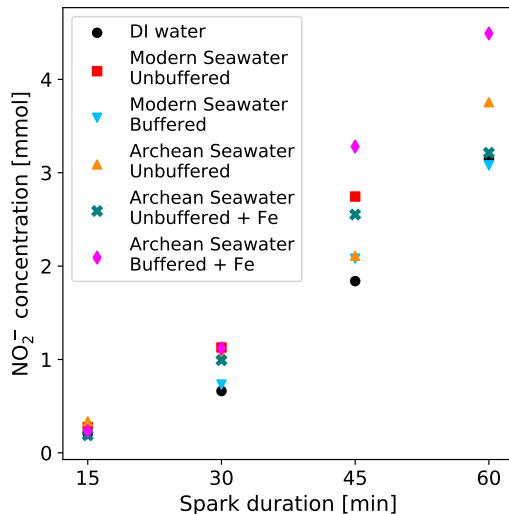


Fig. S9 Nitrite (NO_2^-) concentrations for different durations of spark and different water compositions (Table S1). Starting with 50 ml of water, gas: 0.9 bar N_2 and 0.1 bar CO_2 .

Table S1 Composition of modern and Archean seawater used in experiments⁷⁷ (solvent: DI water). Results presented in Fig. S9.

Compound	Modern seawater	Archean seawater ^a
NaCl	423 mM	423 mM
CaCl ₂	9.27 mM	9.27 mM
MgSO ₄	25.5 mM	-
NaHCO ₃	2.14 mM	2.14 mM
KCl	9 mM	9 mM
CaCO ₃ ^b	1 g	1 g
FeCl ₂ ^c	100 ppm	100 ppm

^a de-oxygenated by pumping N_2 gas through the solution

^b only for buffered seawater

^c only for iron containing seawater

pH was measured. Then 50 ml of the solution were transferred to the reaction flask of the spark discharge experiment, using a syringe. The flask was evacuated and flooded with N_2 gas three times before 0.9 bar N_2 and 0.1 bar CO_2 were added. Finally, the spark generator was turned on. For each liquid composition, four tests were done with discharge times of 15, 30, 45, and 60 min. After the experiment, the liquid in the flask was collected and the yield of nitrite, nitrate, and ammonium were analysed with the colorimetric methods (see above).

The yield of nitrite showed a linear increase with discharge time, from ca. 0.2 mM after 15 min to ca. 3.5 mM after 60 min of sparking (Fig. S9). The minimum yield was found in the experiment with pure water while that the

maximum yield appeared with buffered Archean seawater and iron (for the 60 min experiment). However, the difference among those results is not significant. The nitrate yields, although showing a general increasing trend with reaction time (not shown), are more irregular, likely due to variable degrees of nitrite conversion to nitrate. Ammonium was again several orders of magnitude below nitrite and nitrate concentrations even in the presence of ferrous iron, which can theoretically reduce nitrite and nitrate to ammonium.³⁶

References

- ¹ Postgate, J.R.: Nitrogen Fixation. Cambridge University Press, Cambridge, U.K. (1998)
- ² Fowler, D., Coyle, M., Skiba, U., Sutton, M.A., Cape, J.N., Reis, S., Sheppard, L.J., Jenkins, A., Grizzetti, B., Galloway, J.N., Vitousek, P., Leach, A., Bouwman, A.F., Butterbach-Bahl, K., Dentener, F., Stevenson, D., Amann, M., Voss, M.: The global nitrogen cycle in the twenty-first century. *Philosophical Transactions of the Royal Society B: Biological Sciences* **368**(1621), 20130164 (2013). <https://doi.org/10.1098/rstb.2013.0164>. Publisher: Royal Society
- ³ Beasley, W., Uman, M.A., Rustan Jr., P.L.: Electric fields preceding cloud-to-ground lightning flashes. *Journal of Geophysical Research: Oceans* **87**(C7), 4883–4902 (1982). <https://doi.org/10.1029/JC087iC07p04883>. Publisher: John Wiley & Sons, Ltd
- ⁴ Cavendish, H.: XVII. On the conversion of a mixture of dephlogisticated and phlogisticated air into nitrous acid, by the electric spark. *Philosophical Transactions of the Royal Society of London* **78**, 261–276 (1788). <https://doi.org/10.1098/rstl.1788.0019>. Publisher: Royal Society
- ⁵ Yung, Y.L., McElroy, M.B.: Fixation of Nitrogen in the Prebiotic Atmosphere. *Science* **203**(4384), 1002–1004 (1979). <https://doi.org/10.1126/science.203.4384.1002>
- ⁶ Nna Mvondo, D., Navarro-González, R., McKay, C.P., Coll, P., Raulin, F.: Production of nitrogen oxides by lightning and coronae discharges in simulated early earth, venus and mars environments. *Advances in Space Research* **27**(2), 217–223 (2001). [https://doi.org/10.1016/S0273-1177\(01\)00050-3](https://doi.org/10.1016/S0273-1177(01)00050-3)
- ⁷ Navarro-González, R., McKay, C.P., Mvondo, D.N.: A possible nitrogen crisis for Archean life due to reduced nitrogen fixation by lightning. *Nature* **412**(6842), 61–64 (2001). <https://doi.org/10.1038/35083537>. Publisher: Nature Publishing Group. Accessed 2019-10-01
- ⁸ Summers, D.P., Khare, B.: Nitrogen Fixation on Early Mars and Other Terrestrial Planets: Experimental Demonstration of Abiotic Fixation Reactions

- to Nitrite and Nitrate. *Astrobiology* **7**(2), 333–341 (2007). <https://doi.org/10.1089/ast.2006.0032>. Publisher: Mary Ann Liebert, Inc., publishers
- ⁹ Kasting, J.F., Walker, J.C.G.: Limits on oxygen concentration in the pre-biological atmosphere and the rate of abiotic fixation of nitrogen. *Journal of Geophysical Research* **86**(C2), 1147 (1981). <https://doi.org/10.1029/JC086iC02p01147>. Publisher: John Wiley & Sons, Ltd. Accessed 2019-10-21
- ¹⁰ Wong, M.L., Charnay, B.D., Gao, P., Yung, Y.L., Russell, M.J.: Nitrogen Oxides in Early Earth’s Atmosphere as Electron Acceptors for Life’s Emergence. *Astrobiology* **17**(10), 975–983 (2017). <https://doi.org/10.1089/ast.2016.1473>. Publisher: Mary Ann Liebert, Inc., publishers
- ¹¹ Adams, D., Luo, Y., Wong, M.L., Dunn, P., Christensen, M., Dong, C., Hu, R., Yung, Y.: Nitrogen Fixation at Early Mars. *Astrobiology* **21**(8), 968–980 (2021). <https://doi.org/10.1089/ast.2020.2273>. Publisher: Mary Ann Liebert, Inc., publishers
- ¹² Hoering, T.: The isotopic composition of the ammonia and the nitrate ion in rain. *Geochimica et Cosmochimica Acta* **12**(1), 97–102 (1957). [https://doi.org/10.1016/0016-7037\(57\)90021-2](https://doi.org/10.1016/0016-7037(57)90021-2)
- ¹³ Moore, H.: The isotopic composition of ammonia, nitrogen dioxide and nitrate in the atmosphere. *Atmospheric Environment* (1967) **11**(12), 1239–1243 (1977). [https://doi.org/10.1016/0004-6981\(77\)90102-0](https://doi.org/10.1016/0004-6981(77)90102-0)
- ¹⁴ Shi, G., Ma, H., Zhu, Z., Hu, Z., Chen, Z., Jiang, S., An, C., Yu, J., Ma, T., Li, Y., Sun, B., Hastings, M.G.: Using stable isotopes to distinguish atmospheric nitrate production and its contribution to the surface ocean across hemispheres. *Earth and Planetary Science Letters* **564**, 116914 (2021). <https://doi.org/10.1016/j.epsl.2021.116914>
- ¹⁵ Stüeken, E.E., Kipp, M.A., Koehler, M.C., Buick, R.: The evolution of Earth’s biogeochemical nitrogen cycle. *Earth-Science Reviews* **160**, 220–239 (2016). <https://doi.org/10.1016/j.earscirev.2016.07.007>
- ¹⁶ Stüeken, E.E., Boocock, T., Szilas, K., Mikhail, S., Gardiner, N.J.: Reconstructing Nitrogen Sources to Earth’s Earliest Biosphere at 3.7 Ga. *Frontiers in Earth Science* **9**, 286 (2021). ISBN: 2296-6463
- ¹⁷ Yang, J., Junium, C.K., Grassineau, N.V., Nisbet, E.G., Izon, G., Mettam, C., Martin, A., Zerkle, A.L.: Ammonium availability in the Late Archaean nitrogen cycle. *Nature Geoscience* **12**(7), 553–557 (2019). <https://doi.org/10.1038/s41561-019-0371-1>
- ¹⁸ Marty, B., Zimmermann, L., Pujol, M., Burgess, R., Philippot, P.: Nitrogen Isotopic Composition and Density of the Archean Atmosphere. *Science*

- 342**(6154), 101–104 (2013). <https://doi.org/10.1126/science.1240971>
- ¹⁹ Parker, E.T., Cleaves, J.H., Burton, A.S., Glavin, D.P., Dworkin, J.P., Zhou, M., Bada, J.L., Fernández, F.M.: Conducting Miller-Urey Experiments. *Journal of Visualized Experiments* (83), 51039 (2014). <https://doi.org/10.3791/51039>. Accessed 2019-10-21
- ²⁰ Catling, D.C., Zahnle, K.J.: The Archean atmosphere. *Science Advances* **6**(9), 1420 (2020). <https://doi.org/10.1126/sciadv.aax1420>. Publisher: American Association for the Advancement of Science. Accessed 2020-02-28
- ²¹ Miller, D.N.: Mass transfer in nitric acid absorption. *AIChE Journal* **33**(8), 1351–1358 (1987). <https://doi.org/10.1002/aic.690330812>. Publisher: John Wiley & Sons, Ltd
- ²² Cleaves, H.J., Chalmers, J.H., Lazcano, A., Miller, S.L., Bada, J.L.: A reassessment of prebiotic organic synthesis in neutral planetary atmospheres. *Origins of Life and Evolution of Biospheres* **38**(2), 105–115 (2008). <https://doi.org/10.1007/s11084-007-9120-3>
- ²³ Christian, H.J., Blakeslee, R.J., Boccippio, D.J., Boeck, W.L., Buechler, D.E., Driscoll, K.T., Goodman, S.J., Hall, J.M., Koshak, W.J., Mach, D.M., Stewart, M.F.: Global frequency and distribution of lightning as observed from space by the Optical Transient Detector. *Journal of Geophysical Research: Atmospheres* **108**(D1), 4–1415 (2003). <https://doi.org/10.1029/2002JD002347>. Publisher: John Wiley & Sons, Ltd
- ²⁴ Price, C., Penner, J., Prather, M.: NO_x from lightning: 1. Global distribution based on lightning physics. *Journal of Geophysical Research: Atmospheres* **102**(D5), 5929–5941 (1997). <https://doi.org/10.1029/96JD03504>. Publisher: John Wiley & Sons, Ltd
- ²⁵ Romps, D.M., Seeley, J.T., Vollaro, D., Molinari, J.: Projected increase in lightning strikes in the United States due to global warming. *Science* **346**(6211), 851–854 (2014). <https://doi.org/10.1126/science.1259100>. Publisher: American Association for the Advancement of Science
- ²⁶ Wang, Y., DeSilva, A.W., Goldenbaum, G.C., Dickerson, R.R.: Nitric oxide production by simulated lightning: Dependence on current, energy, and pressure. *Journal of Geophysical Research: Atmospheres* **103**(D15), 19149–19159 (1998). <https://doi.org/10.1029/98JD01356>. Publisher: John Wiley & Sons, Ltd
- ²⁷ Cook, D.R., Liaw, Y.P., Sisterson, D.L., Miller, N.L.: Production of nitrogen oxides by a large spark generator. *Journal of Geophysical Research: Atmospheres* **105**(D6), 7103–7110 (2000). <https://doi.org/10.1029/1999JD901138>. Publisher: John Wiley & Sons, Ltd

- ²⁸ Schumann, U., Huntrieser, H.: The global lightning-induced nitrogen oxides source. *Atmospheric Chemistry and Physics* **7**(14), 3823–3907 (2007). <https://doi.org/10.5194/acp-7-3823-2007>. Accessed 2019-10-24
- ²⁹ Uman, M.A., Rakov, V.A.: Lightning effects on the chemistry of the atmosphere. In: Uman, M.A., Rakov, V.A. (eds.) *Lightning: Physics and Effects*, pp. 507–527. Cambridge University Press, Cambridge (2003). <https://doi.org/10.1017/CBO9781107340886.016>. <https://www.cambridge.org/core/books/lightning/lightning-effects-on-the-chemistry-of-the-atmosphere/6A9292B2B5F1B1979CA38C63AE507000>
- ³⁰ An, T., Yuan, P., Liu, G., Cen, J., Wang, X., Zhang, M., An, Y.: The radius and temperature distribution along radial direction of lightning plasma channel. *Physics of Plasmas* **26**(1), 13506 (2019). <https://doi.org/10.1063/1.5059363>. Publisher: American Institute of Physics
- ³¹ Uman, M.A., Voshall, R.E.: Time interval between lightning strokes and the initiation of dart leaders. *Journal of Geophysical Research* (1896–1977) **73**(2), 497–506 (1968). <https://doi.org/10.1029/JB073i002p00497>. Publisher: John Wiley & Sons, Ltd
- ³² Picone, J.M., Boris, J.P., Greig, J.R., Raleigh, M., Fernsler, R.F.: Convective Cooling of Lightning Channels. *Journal of Atmospheric Sciences* **38**(9), 2056–2062 (1981). [https://doi.org/10.1175/1520-0469\(1981\)038<2056:CCOLC>2.0.CO;2](https://doi.org/10.1175/1520-0469(1981)038<2056:CCOLC>2.0.CO;2). Publisher: American Meteorological Society Place: Boston MA, USA
- ³³ Chameides, W.L.: The Role of Lightning in the Chemistry of the Atmosphere. In: *The Earth’s Electrical Environment*, pp. 70–77. The National Academies Press, Washington, DC (1986). <https://doi.org/10.17226/898>. <https://www.nap.edu/catalog/898/the-earths-electrical-environment>
- ³⁴ Zel’dovich, Y.B., Raizer, Y.P.: *Physics of Shock Waves and High-temperature Hydrodynamic Phenomena*. Academic Press, New York, NY (1966). https://encore.st-andrews.ac.uk/iii/encore/record/C_Rb1169708
- ³⁵ Tosca, N.J., Jiang, C.Z., Rasmussen, B., Muhling, J.: Products of the iron cycle on the early Earth. *Free Radical Biology and Medicine* **140**, 138–153 (2019). <https://doi.org/10.1016/j.freeradbiomed.2019.05.005>
- ³⁶ Summers, D.P., Chang, S.: Prebiotic ammonia from reduction of nitrite by iron (II) on the early Earth. *Nature* **365**(6447), 630–633 (1993). <https://doi.org/10.1038/365630a0>
- ³⁷ Sigman, D.M., Casciotti, K.L., Andreani, M., Barford, C., Galanter, M., Böhlke, J.K.: A Bacterial Method for the Nitrogen Isotopic Analysis of Nitrate in Seawater and Freshwater. *Analytical Chemistry* **73**(17),

- 4145–4153 (2001). <https://doi.org/10.1021/ac010088e>. Publisher: American Chemical Society
- ³⁸ Casciotti, K.L., Sigman, D.M., Hastings, M.G., Böhlke, J.K., Hilkert, A.: Measurement of the Oxygen Isotopic Composition of Nitrate in Seawater and Freshwater Using the Denitrifier Method. *Analytical Chemistry* **74**(19), 4905–4912 (2002). <https://doi.org/10.1021/ac020113w>. Publisher: American Chemical Society
- ³⁹ Walters, W.W., Michalski, G.: Theoretical calculation of nitrogen isotope equilibrium exchange fractionation factors for various NO_y molecules. *Geochimica et Cosmochimica Acta* **164**, 284–297 (2015). <https://doi.org/10.1016/j.gca.2015.05.029>
- ⁴⁰ Kuga, M., Carrasco, N., Marty, B., Marrocchi, Y., Bernard, S., Rigaudier, T., Fleury, B., Tissandier, L.: Nitrogen isotopic fractionation during abiotic synthesis of organic solid particles. *Earth and Planetary Science Letters* **393**, 2–13 (2014). <https://doi.org/10.1016/j.epsl.2014.02.037>. Publisher: Elsevier
- ⁴¹ Li, J., Zhang, X., Orlando, J., Tyndall, G., Michalski, G.: Quantifying the nitrogen isotope effects during photochemical equilibrium between NO and NO₂: implications for $\delta^{15}\text{N}$ in tropospheric reactive nitrogen. *Atmospheric Chemistry and Physics* **20**(16), 9805–9819 (2020). <https://doi.org/10.5194/acp-20-9805-2020>. Accessed 2022-02-02
- ⁴² Walters, W.W., Simonini, D.S., Michalski, G.: Nitrogen isotope exchange between NO and NO₂ and its implications for $\delta^{15}\text{N}$ variations in tropospheric NO_x and atmospheric nitrate. *Geophysical Research Letters* **43**(1), 440–448 (2016). <https://doi.org/10.1002/2015GL066438>. Publisher: John Wiley & Sons, Ltd
- ⁴³ Goldblatt, C., Claire, M.W., Lenton, T.M., Matthews, A.J., Watson, A.J., Zahnle, K.J.: Nitrogen-enhanced greenhouse warming on early Earth. *Nature Geoscience* **2**(12), 891–896 (2009). <https://doi.org/10.1038/ngeo692>
- ⁴⁴ Nijdam, S., Teunissen, J., Ebert, U.: The physics of streamer discharge phenomena. *Plasma Sources Science and Technology* **29**(10), 103001 (2020). <https://doi.org/10.1088/1361-6595/abaa05>. Publisher: IOP Publishing
- ⁴⁵ Rimmer, P.B., Helling, C.: A chemical kinetics network for lightning and life in planetary atmospheres. *The Astrophysical Journal Supplement Series* **224**(1), 9 (2016). <https://doi.org/10.3847/0067-0049/224/1/9>. Publisher: IOP Publishing. Accessed 2019-08-18
- ⁴⁶ Rimmer, P.B., Rugheimer, S.: Hydrogen cyanide in nitrogen-rich atmospheres of rocky exoplanets. *Icarus* **329**, 124–131 (2019). <https://doi.org/10.1016/j.icarus.2019.02.020>

- ⁴⁷ Rimmer, P.B., Helling, C.: Erratum: A Chemical Kinetics Network for Lightning and Life in Planetary Atmospheres. *The Astrophysical Journal Supplement Series* **245**(1), 20 (2019). <https://doi.org/10.3847/1538-4365/ab5192>
- ⁴⁸ Thomazo, C., Papineau, D.: Biogeochemical Cycling of Nitrogen on the Early Earth. *Elements* **9**(5), 345–351 (2013). <https://doi.org/10.2113/gselements.9.5.345>
- ⁴⁹ Ranjan, S., Todd, Z.R., Rimmer, P.B., Sasselov, D.D., Babbin, A.R.: Nitrogen Oxide Concentrations in Natural Waters on Early Earth. *Geochemistry, Geophysics, Geosystems* **20**(4), 2021–2039 (2019). <https://doi.org/10.1029/2018GC008082>. Publisher: John Wiley & Sons, Ltd
- ⁵⁰ Tian, F., Kasting, J.F., Zahnle, K.: Revisiting HCN formation in Earth’s early atmosphere. *Earth and Planetary Science Letters* **308**(3), 417–423 (2011). <https://doi.org/10.1016/j.epsl.2011.06.011>
- ⁵¹ Vinatier, S., Bézard, B., Nixon, C.A.: The Titan ¹⁴N/¹⁵N and ¹²C/¹³C isotopic ratios in HCN from Cassini/CIRS. *Icarus* **191**(2), 712–721 (2007). <https://doi.org/10.1016/j.icarus.2007.06.001>
- ⁵² Niemann, H.B., Atreya, S.K., Demick, J.E., Gautier, D., Haberman, J.A., Harpold, D.N., Kasprzak, W.T., Lunine, J.I., Owen, T.C., Raulin, F.: Composition of Titan’s lower atmosphere and simple surface volatiles as measured by the Cassini-Huygens probe gas chromatograph mass spectrometer experiment. *Journal of Geophysical Research: Planets* **115**(E12) (2010). <https://doi.org/10.1029/2010JE003659>. Publisher: John Wiley & Sons, Ltd. Accessed 2022-10-05
- ⁵³ Weiss, M.C., Sousa, F.L., Mrnjavac, N., Neukirchen, S., Roettger, M., Nelson-Sathi, S., Martin, W.F.: The physiology and habitat of the last universal common ancestor. *Nature Microbiology* **1**(9), 16116 (2016). <https://doi.org/10.1038/nmicrobiol.2016.116>
- ⁵⁴ Stern, J.C., Sutter, B., Freissinet, C., Navarro-González, R., McKay, C.P., Al., E.: Evidence for indigenous nitrogen in sedimentary and aeolian deposits from the Curiosity rover investigations at Gale crater, Mars. *Proceedings of the National Academy of Sciences* **112**(14), 4245–4250 (2015). <https://doi.org/10.1073/pnas.1420932112>. Publisher: Proceedings of the National Academy of Sciences
- ⁵⁵ Sutter, B., McAdam, A.C., Mahaffy, P.R., Ming, D.W., Edgett, K.S., Rampe, E.B., Eigenbrode, J.L., Franz, H.B., Freissinet, C., Grotzinger, J.P., Steele, A., House, C.H., Archer, P.D., Malespin, C.A., Navarro-González, R., Stern, J.C., Bell, J.F., Calef, F.J., Gellert, R., Glavin, D.P., Thompson, L.M., Yen, A.S.: Evolved gas analyses of sedimentary rocks and eolian

- sediment in Gale Crater, Mars: Results of the Curiosity rover's sample analysis at Mars instrument from Yellowknife Bay to the Namib Dune. *Journal of Geophysical Research: Planets* **122**(12), 2574–2609 (2017). <https://doi.org/10.1002/2016JE005225>. Publisher: John Wiley & Sons, Ltd
- ⁵⁶ Cardinal, D., Alleman, L.Y., de Jong, J., Ziegler, K., André, L.: Isotopic composition of silicon measured by multicollector plasma source mass spectrometry in dry plasma mode. *Journal of Analytical Atomic Spectrometry* **18**(3), 213–218 (2003). <https://doi.org/10.1039/B210109B>. Publisher: The Royal Society of Chemistry
- ⁵⁷ NIST Mass Spectrometry Data Center, D. William E. Wallace: Mass Spectra. In: Linstrom, P.J., Mallard, W.G. (eds.) *NIST Chemistry WebBook*, NIST Standard Reference Database Number 69. National Institute of Standards and Technology, Gaithersburg MD, 20899. <https://doi.org/10.18434/T4D303>
- ⁵⁸ Levine, J.S., Hughes, R.E., Chameides, W.L., Howell, W.E.: N₂O and CO production by electric discharge: Atmospheric implications. *Geophysical Research Letters* **6**(7), 557–559 (1979). <https://doi.org/10.1029/GL006i007p00557>. Publisher: John Wiley & Sons, Ltd
- ⁵⁹ Hill, R.D., Rinker, R.G., Coucouvinos, A.: Nitrous oxide production by lightning. *Journal of Geophysical Research: Atmospheres* **89**(D1), 1411–1421 (1984). <https://doi.org/10.1029/JD089iD01p01411>. Publisher: John Wiley & Sons, Ltd
- ⁶⁰ Schnetger, B., Lehnert, C.: Determination of nitrate plus nitrite in small volume marine water samples using vanadium(III)chloride as a reduction agent. *Marine Chemistry* **160**, 91–98 (2014). <https://doi.org/10.1016/j.marchem.2014.01.010>
- ⁶¹ Solórzano, L.: Determination of ammonia in natural waters by the phenol-hypochlorite method *Limnology and Oceanography* **14**(5), 799–801 (1969). <https://doi.org/10.4319/lo.1969.14.5.0799>. Publisher: John Wiley & Sons, Ltd
- ⁶² Böhlke, J.K., Gwinn, C.J., Coplen, T.B.: New reference materials for nitrogen-isotope-ratio measurements. *Geostandards Newsletter* **17**(1), 159–164 (1993)
- ⁶³ Böhlke, J.K., Coplen, T.B.: Interlaboratory comparison of reference materials for nitrogen-isotope-ratio measurements. Technical report, Vienna, Austria (1995). <http://pubs.er.usgs.gov/publication/70188273>
- ⁶⁴ Böhlke, J.K., Mroczkowski, S.J., Coplen, T.B.: Oxygen isotopes in nitrate: new reference materials for 18O:17O:16O measurements and observations

- on nitrate-water equilibration. Rapid communications in mass spectrometry : RCM **17**(16), 1835–1846 (2003). <https://doi.org/10.1002/rcm.1123>. Place: England
- ⁶⁵ Li, L., Lollar, B.S., Li, H., Wortmann, U.G., Lacrampe-Couloume, G.: Ammonium stability and nitrogen isotope fractionations for NH₄⁺–NH₃(aq)–NH₃(gas) systems at 20–70°C and pH of 2–13: Applications to habitability and nitrogen cycling in low-temperature hydrothermal systems. *Geochimica et Cosmochimica Acta* **84**, 280–296 (2012). <https://doi.org/10.1016/j.gca.2012.01.040>
- ⁶⁶ Woitke, P., Helling, C., Hunter, G.H., Millard, J.D., Turner, G.E., Worters, M., Bleicic, J., Stock, J.W.: Equilibrium chemistry down to 100 K - Impact of silicates and phyllosilicates on the carbon to oxygen ratio,. *Astronomy & Astrophysics* **614**, 1 (2018). <https://doi.org/10.1051/0004-6361/201732193>. Publisher: EDP Sciences. Accessed 2022-10-19
- ⁶⁷ Joshi, J.B., Mahajani, V.V., Juvekar, V.A.: Absorption of NO_x Gases. *Chemical Engineering Communications* **33**(1-4), 1–92 (1985). <https://doi.org/10.1080/00986448508911161>. Publisher: Taylor & Francis
- ⁶⁸ Levine, J.S., Rogowski, R.S., Gregory, G.L., Howell, W.E., Fishman, J.: Simultaneous measurements of NO_x, NO, and O₃ production in a laboratory discharge: Atmospheric implications. *Geophysical Research Letters* **8**(4), 357–360 (1981). <https://doi.org/10.1029/GL008i004p00357>. Publisher: John Wiley & Sons, Ltd
- ⁶⁹ Stark, M.S., Harrison, J.T.H., Anastasi, C.: Formation of nitrogen oxides by electrical discharges and implications for atmospheric lightning. *Journal of Geophysical Research: Atmospheres* **101**(D3), 6963–6969 (1996). <https://doi.org/10.1029/95JD03008>. Publisher: John Wiley & Sons, Ltd
- ⁷⁰ Summers, D.P., Basa, R.C.B., Khare, B., Rodoni, D.: Abiotic Nitrogen Fixation on Terrestrial Planets: Reduction of NO to Ammonia by FeS. *Astrobiology* **12**(2), 107–114 (2012). <https://doi.org/10.1089/ast.2011.0646>. Publisher: Mary Ann Liebert, Inc., publishers
- ⁷¹ Zuo, Y., Deng, Y.: Evidence for the production of hydrogen peroxide in rain-water by lightning during thunderstorms. *Geochimica et Cosmochimica Acta* **63**(19), 3451–3455 (1999). [https://doi.org/10.1016/S0016-7037\(99\)00274-4](https://doi.org/10.1016/S0016-7037(99)00274-4)
- ⁷² Bunton, C.A., Llewellyn, D.R., Stedman, G.: 116. Oxygen exchange between nitrous acid and water. *Journal of the Chemical Society (Resumed)* (0), 568–573 (1959). <https://doi.org/10.1039/JR9590000568>. Publisher: The Royal Society of Chemistry
- ⁷³ McIlvin, M.R., Casciotti, K.L.: Method for the Analysis of $\delta^{18}\text{O}$ in Water.

- Analytical Chemistry **78**(7), 2377–2381 (2006). <https://doi.org/10.1021/ac051838d>. Publisher: American Chemical Society
- ⁷⁴ Newman, B.L., Carta, G.: Mass transfer in the absorption of nitrogen oxides in alkaline solutions. *AIChE Journal* **34**(7), 1190–1199 (1988). <https://doi.org/10.1002/aic.690340715>. Publisher: John Wiley & Sons, Ltd
- ⁷⁵ Köhn, C., Ebert, U.: Calculation of beams of positrons, neutrons, and protons associated with terrestrial gamma ray flashes. *Journal of Geophysical Research: Atmospheres* **120**(4), 1620–1635 (2015). <https://doi.org/10.1002/2014JD022229>. Publisher: John Wiley & Sons, Ltd
- ⁷⁶ Köhn, C., Dujko, S., Chanrion, O., Neubert, T.: Streamer propagation in the atmosphere of Titan and other N₂:CH₄ mixtures compared to N₂:O₂ mixtures. *Icarus* **333**, 294–305 (2019). <https://doi.org/10.1016/j.icarus.2019.05.036>
- ⁷⁷ Henson, J.H., Samasa, B., Burg, E.C.: Chapter 17 - High resolution imaging of the cortex isolated from sea urchin eggs and embryos. In: Hamdoun, A., Foltz, K.R.B.T.-M.i.C.B. (eds.) *Echinoderms, Part B* vol. 151, pp. 419–432. Academic Press, Cambridge, MA (2019). <https://doi.org/10.1016/bs.mcb.2019.01.005>. <https://www.sciencedirect.com/science/article/pii/S0091679X19300056>